 CMES, vol.77, no.1, pp.1-31, 2011

Application of Meshless Local Petrov-Galerkin (MLPG) Method to Three Dimensional Elasto-Plastic Problems Based on Deformation Theory of Plasticity

A. Rezaei Mojdehi[1,2], A. Darvizeh[3] and A. Basti[2]

Abstract: In this paper, a meshless method based on the local petrov-galerkin approach is proposed for the three dimensional (3D) elasto-plastic problems. Galerkin weak-form formulation is applied to derive the discrete governing equations. A weak formulation for the set of governing equations is transformed into local integral equations on local sub-domains by using a unit test function. Nodal points are distributed in the 3D analyzed domain and each node is surrounded by a cubic sub-domain to which a local integral equation is applied. Three dimensional Moving Least-Square (MLS) approximation is used as shape function to approximate the field variable of scattered nodes in the problem domain. Hencky's total deformation theory is used to define effective elastic material parameters, which are treated as spatial field variables and considered as functions of the equilibrium stress state and material properties. These effective material parameters are obtained in an iterative process. Several example problems are presented to illustrate the effectiveness of the numerical approach.

Keywords: Meshless Local Petrov-Galerkin method, Elasto-Plastic Analysis, Hencky's Total Deformation Theory, Three Dimensional Moving Least Square approximation.

1 Introduction

Due to nonlinear nature of materials in the engineering structures, it is very important to consider this aspect of analysis in solving engineering problems. However, the nonlinear stress–strain relationship and the loading path dependency in the plastic range make the analysis tedious. From the viewpoint of mathematics, the discretization of nonlinear problems results a set of simultaneous equations, in which

[1] Wind Turbines Technology Development Center, Niroo Research Institute, Tehran, Iran
[2] Department of Mechanical engineering, Faculty of Engineering, The University of Guilan, Iran
[3] Department of Mechanical Engineering, Faculty of Engineering, Islamic Azad University, Anzali Branch, Bandar-e Anzali, Iran

equation coefficients depend on the solutions variable or their derivatives. Due to the mathematical difficulties, analytical solutions are limited to problems with very simple geometries and external loadings. Consequently, approximate solutions of realistic engineering problems are usually obtained numerically. Numerical techniques with different discretization schemes, such as FEM, have been widely used for the analysis of material behaviour in the elastic and elasto-plastic ranges, especially in practical engineering applications [Belytschko, Liu and Moran (2000); Zienkiewicz and Taylor (2000)] . However, mesh based finite element method faces difficulties in solving problems involving large deformation and discontinuities, such as mesh distortion, crack propagation and the growth of phase boundaries. In those problems, in order to maintain the element connectivity, high computational cost is involved in the mesh generation and refinement algorithms. To overcome these shortcomings, the concept of meshless method has been proposed.

During recent years, meshless approaches have attracted considerable attention due to their capability to solve a boundary value problem without a meshing procedure. In contrast to the finite element formulation, computational model is described only by a set of nodes which don't need to be connected into elements. Thus, the nodes can be easily added and removed without burdensome remeshing of the entire structure. Furthermore, by using the meshless formulation many other difficulties associated with the finite element method may also be overcome. A variety of these methods have been developed which include Element-Free Galerkin method [Belytschko, Lu and Gu (1994)] , the reproducing kernel particle method [Liu, W. K., Jun and Zhang (1995)] , hp-clouds [Duarte and Oden (1996)] , the partition of unity method [Babuska and Melenk (1997)] , meshless Galerkin using radial basis functions [Wendland (1995)] , the diffuse element [Nayroles, Touzot and Villon (1992)] , the natural element [Sukumar, Moran and Belytschko (1998)] , the smoothed particle hydrodynamics [Lucy (1977)] , the collocation technique employing radial basis functions [Fasshauer (1997)] and the modified smoothed particle hydrodynamics [Zhang, G. M. and Batra (2004)] . Of these, the last three methods do not require any mesh whereas others generally need a background mesh for the evaluation of integrals appearing in the weak formulation of the problem.

Up to now, most developments in meshless methods have been focused mainly on linear elastic materials. Research in inelastic or elasto-plasticity materials using meshless methods has not been widespread and is only gaining attention recently. Currently, application of meshless methods in plasticity problems are mainly focused on the element-free Galerkin (EFG) and reproducing kernel particle methods. Rao and Rahman (2004) proposed an enriched meshless method for fracture analysis of mode-I crack in non-linear elastic, two dimensional solids. It involves an EFG method and two new enriched basis functions to analysis of non-linear

fracture mechanics. Kargarnovin et al. (2004) extended the EFG method to elasto-plastic stress analysis using the incremental formulation of plastic deformation. Xu and Saigal [(1998); (1999)] proposed an EFG based formulation for steady quasi-static and dynamic crack growth, in elasto-plastic materials undergoing small scale yielding. Chen et al. (2002) formulated the dynamic meshless methods for local and non-local field theories and applied the method to two crack problems. Liu et al. (2006) employed an element-free Galerkin-finite element coupling method to solve elasto-plastic contact problems. Belinha and Dinis (2006) carried out elasto-plastic analysis of plates using the element-free Galerkin method. Jianfeng et al. (2008) extended meshless integral method based on regularized boundary integral equation to elasto-plastic materials. Chen et al.(1996) implemented reproducing kernel particle method (RKPM) to model large deformation analysis of nonlinear structures. Liew et al.(2002) proposed an RKPM algorithm based on parametric programming for elasto plasticity problems. Li et al. (2000) performed large deformation analysis of thin shell structures using RKPM.

The Meshless Local Petrov–Galerkin (MLPG) method developed by Atluri et al. [(1998); (1999); (2002b); (2002a)] is a truly meshless method which is based on the local weak rather than the global weak formulation of the problem, and does not require a background mesh for the evaluation of integrals in the weak formulation of the problem. In the MLPG method, the trial and test functions are chosen from totally different functional spaces. Furthermore, the physical size of the test and trial domains is not necessary to be the same, which makes the MLPG a very flexible method. Based on the concept of the MLPG, six different methods have been introduced, which are labeled as MLPG1–MLPG6 Atluri and Shen (2002b) . Difference between These six methods is due to the type of test function considered in the weak formulation. The MLPG methods have been employed in a wide range of applications, for example elasto-statics [Atluri and Zhu (2000)] , elasto-dynamics [Batra and Ching (2002)] , fluid mechanics [Lin and Atluri (2001)] , convection–diffusion problems [Lin and Atluri (2000)] , thermoelasticity [Sladek, Sladek and Atluri (2001)] , beam problems [Atluri, Cho and Kim (1999); Gu and Liu (2001)] , plate problems [Gu and Liu (2001); Long, S. and Atluri (2002); Qian, L. F, Batra and Chen (2003); Soric, Li, Jarak and Atluri (2004); Li, Q., Soric, Jarak and Atluri (2005); Sladek, Sladek, Krivacek, Wen and Zhang (2007); Xiao, Batra, Gilhooley, Gillespie Jr. and McCarthy (2007)] , fracture mechanics [Kim and Atluri (2000); Ching and Batra (2001)] , strain gradient theory [Tang, Shen and Atluri (2003)] and FGM problems [Qian, L. F., Batra and Chena (2004); Ching and Yen (2005); Sladek, sladek and Zhang (2005); Ching and Yen (2006); Gilhooley, Batra, Xiao, McCarthy and Gillespie Jr. (2007); Sladek, Sladek and Solek (2009); Rezaei Mojdehi, Darvizeh, Basti and Rajabi (2011)] . All of these wide ranges

of applications demonstrate that the MLPG method is one of the most promising alternative methods for computational mechanics.

There are a few works carried out with MLPG method for analysis of elasto-plastic materials and material nonlinearities; Han et al. (2005) developed MLPG mixed finite volume method for the large deformation analysis of static and dynamic problems with application to high speed impact problems. Zhang et al. (2006) presented two-dimensional large deformation analysis of hyperelastic and elasto-plastic materials based on MLPG method. Gu et al. (2007) extended MLPG method for two-dimensional analysis of material nonlinear problems based on deformation theory of plasticity. Long et al. (2008) developed MLPG method for elasto-plastic fracture problems. Soares et al. (2009) presented analyze of dynamic problems containing one example with elasto-plasticity. Except first one, which is a mixed approach, all of mentioned papers are limited to the two-dimensional problems. After many pioneering research studies were successfully carried out for 2D problems, the MLPG methods are becoming more attractive for solving 3D problems, because of their distinct advantages over the element-based methods. The representative 3D works, include the papers [Han and Atluri (2003); Li, Q., Shen, Han and Atluri (2003); Han and Atluri (2004b); (2004a); Sladek, Sladek and Solek (2009); Rezaei Mojdehi, Darvizeh, Basti and Rajabi (2011)] for elastic problems by using the MLPG domain methods. It has been reported that the MLPG methods give better accuracy with lesser CPU time and lesser system resources, than the element-based methods [Atluri and Shen (2002b); (2002a); Han and Atluri (2004b)] .

In the present work, meshless local petrov-galerkin method is developed for the 3D elasto-plastic problems. Galerkin weak-form formulation is applied to derive the discrete governing equilibrium equations in a three dimensional continuum. Numerical integration is performed using Gauss quadrature method. A weak formulation for the set of governing equations is transformed into local integral equations on local sub-domains by using a unit test function. Nodal points are distributed in the 3D analyzed domain and each node is surrounded by a cubic sub-domain to which a local integral equation is applied. Three dimensional Moving Least-Square (MLS) approximation is used as shape function to approximate the field variable of scattered nodes in the problem domain. Hencky's total deformation theory is used to define stress-strain relations in the plastic zones. Effective elastic material parameters, which are treated as spatial field variables and considered as functions of the equilibrium stress state and material properties, are obtained from effective constitutive equations of elasto-plastic materials. These effective material parameters are obtained in an iterative process based on strain controlled projection method, using experimental uniaxial tension test curve. The supports of the MLS approximation function cover the same sets of nodes during iterative procedures, thus the

shape function need to be computed only in the initial stage. Von Mises yield criterion in three dimensional space is used as a yield function to distinguish plastic zone from elastic one. Several numerical examples are presented to illustrate the effectiveness of the present formulation. The obtained results from present method have been compared with those of finite element commercial software ABAQUS and are found to be in good agreement with them.

2 MLPG formulation for 3D problems

Consider the problem of three-dimensional linear elasticity, where the equilibrium equations in a domain of the volume Ω, which is bounded by the surface Γ, are given by;

$$_{ij,j} + b_i = 0, \qquad \text{in } \Omega \tag{1}$$

where $_{ij,j}$ are the components of the symmetric stress tensor which correspond to the displacement field u_i and b_i are the body force. The indices *i, j* which take the values 1, 2 and 3 refer to the coordinates *x, y, z* on the boundary Γ, respectively. A comma followed by index *j* denotes partial differentiation with respect to the position $\mathbf{x}^j$ of a material particle. The following boundary conditions are assumed;

$$u_i = \overline{u}_i, \qquad on \ \ \Gamma_u \tag{2a}$$

$$t_i = \sigma_{ij} n_j = \bar{t}_i, \qquad on \ \ \Gamma_t \tag{2b}$$

where $\overline{u}_i$ and $\bar{t}_i$ are the prescribed displacements and surface tractions, on the displacement boundary Γ_u and on the traction boundary Γ_t , respectively. n_j are the components of a unit outward normal to the global boundary Γ.

The weak form of governing equations can be obtained over the local sub-domains, which are located entirely inside the global domain Ω. The local sub-domains may overlap with each other and must cover the whole global domain. Various arbitrary shapes, with different sizes, such as spheres, cubes and ellipsoids can be chosen as sub-domains in 3D domains. In the present work, cubic domains are considered as local sub-domain and support domain which can be seen in Fig. 1.

2.1 Local weak form of 3D solids

Based on the local petrov-galerkin approaches, a generalized local weak form of the equilibrium equation over a local sub-domain Ω_q, can be written as;

$$\int_{\Omega_q} (\sigma_{ij,j} + b_i)\, v_i d\Omega - \alpha \int_{\Gamma_{qu}} (u_i - \overline{u}_i)\, v_i d\Gamma = 0 \tag{3}$$

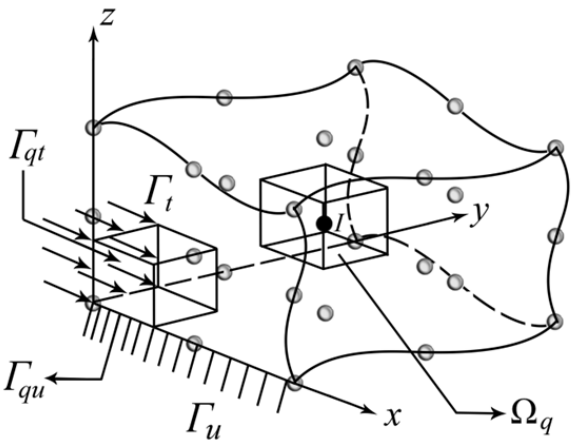

Figure 1: Local sub-domains used in the MLPG method

herein u_i is the trial function describing the displacement field, while v_i is the test function. α denotes a penalty parameter, $\alpha \gg 1$, which is introduced in order to satisfy the essential boundary conditions.

Unlike the conventional Galerkin method in which the trial and test functions are chosen from the same space, the Petrov-Galerkin method uses the trial and the test functions from different spaces. In particular, the test functions don't need to vanish on the boundary where the essential boundary conditions are specified. By applying the divergence theorem from Eq. 4, Eq. 3 may be rewritten as;

$$\sigma_{ij,j} v_i = \left(\sigma_{ij} v_i\right)_{,j} - \sigma_{ij} v_{i,j} \tag{4}$$

$$\int_{\Gamma_q} \sigma_{ij} n_j v_i d\Gamma - \int_{\Omega_q} \left(\sigma_{ij} v_{i,j} - b_i v_i\right) d\Omega - \alpha \int_{\Gamma_{qu}} \left(u_i - \overline{u}_i\right) v_i d\Gamma = 0 \tag{5}$$

by imposing the natural boundary conditions in Eq. 2b one obtains;

$$\int_{\Gamma_{qi}} t_i v_i d\Gamma + \int_{\Gamma_{qu}} t_i v_i d\Gamma + \int_{\Gamma_{qt}} \overline{t}_i v_i d\Gamma - \int_{\Omega_q} \left(\sigma_{ij} v_{i,j} - b_i v_i\right) d\Omega - \alpha \int_{\Gamma_{qu}} \left(u_i - \overline{u}_i\right) v_i d\Gamma = 0 \tag{6}$$

As evident, the boundary Γ_q of the local sub-domain is divided into three parts, i.e., $\Gamma_q = \Gamma_{qi} \cup \Gamma_{qu} \cup \Gamma_{qt}$, in which Γ_{qi} is the internal boundary of the local sub-domain, which does not intersect with the global boundary Γ; Γ_{qt} is the part of the natural boundary that intersects with the local sub-domain and Γ_{qu} is the part of

the essential boundary that intersects with the local sub-domain. Fig. 1, shows the local sub-domain used in the MLPG method.

Eq. 6 can be rewritten as;

$$\int_{\Omega_q} \sigma_{ij} v_{i,j} d\Omega - \int_{\Gamma_{qi}} t_i v_i d\Gamma - \int_{\Gamma_{qu}} t_i v_i d\Gamma + \alpha \int_{\Gamma_{qu}} u_i v_i d\Gamma = \int_{\Gamma_{qt}} \bar{t}_i v_i d\Gamma + \alpha \int_{\Gamma_{qu}} \bar{u}_i v_i d\Gamma + \int_{\Omega_q} b_i v_i d\Omega \quad (7)$$

which represent a set of three equations for each local sub-domain. In the present implementation, the local domain is chosen as a cube, centered at a node $\mathbf{x}_i$. The test function v_i is chosen such that it is positive inside the local sub-domain Ω_q and vanishes outside of Ω_q.

2.2 3D approximation using Moving Least Square (MLS) approximation

Using the MLS shape functions, we can approximate the trial function for the displacement at each point. The MLS approximation of $u(\mathbf{x})$ is defined at $\mathbf{x}$ as;

$$u^h(\mathbf{x}) = \sum_{i=1}^{m} p_i(\mathbf{x}) a_i(\mathbf{x}) = \mathbf{p}^{\mathrm{T}}(\mathbf{x}) \mathbf{a}(\mathbf{x}) \qquad \forall \mathbf{x} \in \Omega \quad (8)$$

where $\mathbf{p}^T(\mathbf{x}) = [p_1(\mathbf{x}), p_2(\mathbf{x}), \ldots, p_m(\mathbf{x})]$ is a vector of complete basis functions of order m and $\mathbf{a}(\mathbf{x})$ is a vector containing the coefficients $a_i(\mathbf{x})$, $i = 1, 2, \ldots, m$, which are functions of the space coordinates $\mathbf{x} = [x, y, z]^T$. In 3D problems, the linear basis is defined as;

$$\mathbf{p}^{\mathrm{T}}(\mathbf{x}) = [1, x, y, z]; \quad m = 4 \quad (9)$$

and the quadratic basis is defined as;

$$\mathbf{p}^{\mathrm{T}}(\mathbf{x}) = \left[1, x, y, z, x^2, y^2, z^2, xy, yz, xz\right]; \quad m = 10 \quad (10)$$

The coefficient vector function $a_i(\mathbf{x})$ is determined by minimizing a weighted discrete L_2 norm, which is defined as;

$$J(\mathbf{x}) = \sum_{I=1}^{N} \mathrm{w}_I(\mathbf{x}) \left[\mathbf{p}^{\mathrm{T}}(\mathbf{x}_I)\mathbf{a}(\mathbf{x}) - \hat{u}^I\right]^2 \quad (11)$$

where $\hat{u}^I$ are the fictitious nodal values and w_I is the weight function associated with the node I. N is the number of nodes in the support domain for which the weight function $\mathrm{w}_I(\mathbf{x}) > 0$ and $\mathbf{x}_I$ denotes the value of $\mathbf{x}$ at nod I. A fourth-order

spline weight function is considered in the present work. This weight function corresponding to node I for a one-dimensional domain may be written as;

$$w_I(x) = \begin{cases} 1-6\left(\frac{d_I(x)}{r_I(x)}\right)^2+8\left(\frac{d_I(x)}{r_I(x)}\right)^3-3\left(\frac{d_I(x)}{r_I(x)}\right)^4 & 0 \le d_I(x) \le r_I(x) \\ 0 & d_I(x) > r_I(x) \end{cases} \tag{12}$$

where $d_I(x) = x - x_I$ is the distance from node $\mathbf{x}_I$ to point $\mathbf{x}$ in x direction; while $r_I(x)$ is the size of the support for the weight function $w_I(x)$ defined as $r_I(x) = \alpha_s d_I(x)$ which the weight function $w_I(x)$ associated with node $\mathbf{x}_I$ is non-zero and α_s is the dimensionless size of the support domain. Using the cubic support domain, the weight function for the 3D problem can be obtained by a simple extension of the one-dimensional function of Eq. 12 as follows;

$$\mathrm{w}_I(\mathbf{x}) = \mathrm{w}_I(x,y,z) = w_I(x)\, w_I(y)\, w_I(z) \tag{13}$$

where functions $w_I(y)$ and $w_I(z)$ are obtained by replacing x with y and z in Eq. 12, respectively. In this regard, the parameters $d_I(y) = y - y_I$ and $d_I(z) = z - z_I$ are the distances from node $\mathbf{x}_I$ to point $\mathbf{x}$ in y and z direction, respectively.

The stationary condition of J in Eq. 11 with respect to $\mathbf{a}(\mathbf{x})$,

$$\partial J / \partial \mathbf{a} = 0 \tag{14}$$

leads to the following linear relation between fictitious ($\widehat{\mathbf{u}}$) and approximated (u^h) nodal displacements.

$$u^h(\mathbf{x}) = \int_{I=1}^{N} \Phi^I(\mathbf{x})\, \hat{u}^I = \Phi^{\mathrm{T}}(\mathbf{x})\, \widehat{\mathbf{u}} \tag{15}$$

where $\Phi^T(\mathbf{x})$ can then be described as the shape function associated with the nodes and is given as;

$$\Phi^T(\mathbf{x}) = \mathbf{P}^{\mathrm{T}}(\mathbf{x})\, \mathbf{A}^{-1}(\mathbf{x})\, \mathbf{B}(\mathbf{x}) \tag{16}$$

where,

$$\mathbf{A}(\mathbf{x}) = \int_{I=1}^{N} \mathrm{w}_I(\mathbf{x}) \mathbf{p}(\mathbf{x}_I)\, \mathbf{p}^{\mathrm{T}}(\mathbf{x}_I) = \mathbf{P^T W} P \tag{17}$$

$$\mathbf{B}(\mathbf{x}) = [\mathrm{w}_1(\mathbf{x})\, \mathbf{p}(\mathbf{x}_1),\ \mathrm{w}_2(\mathbf{x})\, \mathbf{p}(\mathbf{x}_2),\ \ldots,\ \mathrm{w}_N(\mathbf{x})\, \mathbf{p}(\mathbf{x}_{\mathrm{N}})] = \mathbf{P^T W} \tag{18}$$

herein,

$$\mathbf{P} = \begin{bmatrix} \mathbf{p}^{\mathrm{T}}(\mathbf{x}_1) \\ \mathbf{p}^{\mathrm{T}}(\mathbf{x}_2) \\ \vdots \\ \mathbf{p}^{\mathrm{T}}(\mathbf{x}_{\mathrm{N}}) \end{bmatrix}_{N\times m} \tag{19}$$

and,

$$\mathbf{W} = \begin{pmatrix} \mathrm{w}_1(\mathbf{x}) & \cdots & 0 \\ \vdots & \ddots & \vdots \\ 0 & \cdots & \mathrm{w}_N(\mathbf{x}) \end{pmatrix}_{N\times N} \tag{20}$$

The partial derivatives of the trial function are introduced as follows;

$$u^h_{,x}(\mathbf{x}) = \int_{I=1}^{N} \Phi^I_{,x}(\mathbf{x})\,\hat{u}^I \tag{21}$$

where $\Phi^I_{,x}$ are derivatives of the MLS shape function and can be obtained as;

$$[\Phi^I_{,x}(\mathbf{x}) = \int_{j=1}^{m} \left[p_{j,x}\left(\mathbf{A}^{-1}\mathbf{B}\right)_{jI} + p_j\left(\mathbf{A}^{-1}\mathbf{B}_{,x} + \mathbf{A}^{-1}_{,x}\mathbf{B}\right)_{jI}\right] \tag{22}$$

where $\mathbf{A}^{-1}_{,x} = -\mathbf{A}^{-1}\mathbf{A}_{,x}\mathbf{A}^{-1}$ represents the derivative of the inverse of matrix $\mathbf{A}$ with respect to x.

2.3 Test function

Atluri and Shen (2002b) have proposed six different choices for test functions and labeled the corresponding formulations as MLPG1 through MLPG6. Here we take the test function to be a fourth-order spline weight function. The corresponding MLPG formulation is called MLPG1. Cubic sub-domain is also chosen for the support of the test function. The test function for the cubic sub-domain is constructed following the same procedure as mentioned in the previous section for constructing the weight function. Therefore, the test function for MLPG1 is defined as;

$$v_I(\mathbf{x}) = v_I(x)\,v_I(y)\,v_I(z) = \begin{cases} 1 - 6\left(\frac{d_I(\mathbf{x})}{r_q(\mathbf{x})}\right)^2 + 8\left(\frac{d_I(\mathbf{x})}{r_q(\mathbf{x})}\right)^3 - 3\left(\frac{d_I(\mathbf{x})}{r_q(\mathbf{x})}\right)^4 & 0 \le d_I(\mathbf{x}) \le r_q(\mathbf{x}) \\ 0 & d_I(\mathbf{x}) > r_q(\mathbf{x}) \end{cases} \tag{23}$$

where $d_I = \mathbf{x} - \mathbf{x}_I$ and $r_q(\mathbf{x})$ is the size of the support for the test function v_I defined as $r_q(\mathbf{x}) = \alpha_q d_I(\mathbf{x})$ which the test function $v_I(\mathbf{x})$ associated with node $\mathbf{x}_I$ is non-zero and α_q is the dimensionless size of the support for the test function domain.

2.4 Discretization and numerical implementation

The geometry of the problem is discretized by the nodes located on the 3D problem domain. By using, the test function, in the MLPG method, only three linear equations of $\hat{u}$ will yield for each point and/or its local domains. Note that the trial function u within the sub-domain Ω_q, in MLS approximation, is determined by the fictitious nodal values $\hat{u}_i$, in the domain of definition for all points $\mathbf{x}$ falling in Ω_q. The nodal variables are three fictitious displacement components in the Cartesian coordinate system *x, y, z*. Therefore, we need as many local domains Ω_q as the number of nodes in the global domain to obtain as many equations as the number of unknowns.

The stress tensor components σ_{ij} can be written in a Cartesian coordinate system as;

$$\sigma^T = [\sigma_x \;\; \sigma_y \;\; \sigma_z \;\; xy \;\; yz \;\; zx] \tag{24}$$

Using an effective material parameter in a generalized Hooke's law, the stress tensor components in elastic and plastic phase can be expressed in terms of the nodal unknown variables by the relation;

$$\sigma = \int_{j=1}^{N} \mathbf{D}_e \mathbf{B}_j \mathbf{u}_j \tag{25}$$

where $\mathbf{D}_e$ is the three-dimensional effective material parameter which is a function of the equilibrium stress state and material properties in plastic phase and is constant in elastic one. $\mathbf{B}_j$ denotes the strain-displacement matrix obtained by differentiation of the shape function in a three dimensional space;

$$\mathbf{D}_e = {D_0}^e \begin{bmatrix} 1 & \frac{\nu_e}{1-\nu_e} & \frac{\nu_e}{1-\nu_e} & 0 & 0 & 0 \\ \frac{\nu_e}{1-\nu_e} & 1 & \frac{\nu_e}{1-\nu_e} & 0 & 0 & 0 \\ \frac{\nu_e}{1-\nu_e} & \frac{\nu_e}{1-\nu_e} & 1 & 0 & 0 & 0 \\ 0 & 0 & 0 & \frac{1-2\nu_e}{2(1-\nu_e)} & 0 & 0 \\ 0 & 0 & 0 & 0 & \frac{1-2\nu_e}{2(1-\nu_e)} & 0 \\ 0 & 0 & 0 & 0 & 0 & \frac{1-2\nu_e}{2(1-\nu_e)} \end{bmatrix} \tag{26}$$

$${D_0}^e = \frac{E_e\,(1-\nu_e)}{(1+\nu_e)\,(1-2\nu_e)} \tag{27}$$

where E_e and ν_e are effective Young's modulus and Poisson's ratio, which are ob-

tained from iterative projection technique and will be discussed in the next Sections.

$$\mathbf{B}_{(6\times 3N)} = \begin{bmatrix} \frac{\partial \Phi_1}{\partial x} & 0 & 0 & \dots & \frac{\partial \Phi_N}{\partial x} & 0 & 0 \\ 0 & \frac{\partial \Phi_1}{\partial y} & 0 & \dots & 0 & \frac{\partial \Phi_N}{\partial y} & 0 \\ 0 & 0 & \frac{\partial \Phi_1}{\partial z} & \dots & 0 & 0 & \frac{\partial \Phi_N}{\partial z} \\ \frac{\partial \Phi_1}{\partial y} & \frac{\partial \Phi_1}{\partial x} & 0 & \dots & \frac{\partial \Phi_N}{\partial y} & \frac{\partial \Phi_N}{\partial x} & 0 \\ 0 & \frac{\partial \Phi_1}{\partial z} & \frac{\partial \Phi_1}{\partial y} & \dots & 0 & \frac{\partial \Phi_N}{\partial z} & \frac{\partial \Phi_N}{\partial y} \\ \frac{\partial \Phi_1}{\partial z} & 0 & \frac{\partial \Phi_1}{\partial x} & \dots & \frac{\partial \Phi_N}{\partial z} & 0 & \frac{\partial \Phi_N}{\partial x} \end{bmatrix} \tag{28}$$

The surface traction components $\mathbf{t}$ may also be expressed in a vector form by the relation;

$$\mathbf{t} = \mathbf{N}\sigma = \int_{j=1}^{N} \mathbf{N}D\mathbf{B}_j\mathbf{u}_j \tag{29}$$

which $\mathbf{N}$ is the matrix describing the outward normal on Γ_q,

$$\mathbf{N} = \begin{bmatrix} n_x & 0 & 0 & n_y & 0 & n_z \\ 0 & n_y & 0 & n_x & n_z & 0 \\ 0 & 0 & n_z & 0 & n_y & n_x \end{bmatrix} \tag{30}$$

By substituting fourth-order spline test function from Eq. 23 into Eq. 7 and by means of Eqs. 15, 25 and 29, Eq. 7 is transformed in the discretized system of equations which may be written in the matrix form as;

$$\mathbf{K}u = \mathbf{F} \tag{31}$$

where, $\mathbf{K}$ and $\mathbf{F}$ are equivalent stiffness and force matrixes, respectively, i.e.

$$\mathrm{K_{ij}} = \int_{\Omega_q} \left(\widehat{\mathbf{W}}_i^T \mathbf{D}_e \mathbf{B}_j\right) d\Omega - \int_{\Gamma_{qi}} \mathbf{V}_i \mathbf{N}\mathbf{D}_e\mathbf{B}_j d\Gamma - \int_{\Gamma_{qu}} \mathbf{V}_i \mathbf{N}\mathbf{D}_e\mathbf{B}_j d\Gamma + \alpha \int_{\Gamma_{qu}} \mathbf{V}_i \Phi_j d\Gamma \tag{32}$$

$$\mathrm{F_{ij}} = \int_{\Gamma_{qt}} \bar{t}_i \mathbf{V}_i d\Gamma + \alpha \int_{\Gamma_{qu}} \overline{u}_i \mathbf{V}_i d\Gamma + \int_{\Omega_q} b_i \mathbf{V}_i d\Omega \tag{33}$$

where $\widehat{\mathbf{W}}_i$, b_i and $\bar{t}_i$ are the test function derivatives, body force and traction matrices, corresponding to node i, respectively.

where,

$$\mathbf{V}_i = \begin{bmatrix} \nu(\mathbf{x}, \mathbf{x}_\mathrm{i}) & 0 & 0 \\ 0 & \nu(\mathbf{x}, \mathbf{x}_\mathrm{i}) & 0 \\ 0 & 0 & \nu(\mathbf{x}, \mathbf{x}_\mathrm{i}) \end{bmatrix} \tag{34}$$

$$\widehat{\mathbf{W}}_i = \begin{bmatrix} v_{,x} & 0 & 0 & v_{,y} & 0 & v_{,z} \\ 0 & v_{,y} & 0 & v_{,x} & v_{,z} & 0 \\ 0 & 0 & v_{,z} & 0 & v_{,y} & v_{,x} \end{bmatrix} \tag{35}$$

Equations similar to Eq. 31 with stiffness and force matrix (as Eqs. 32 and 33) are obtained for each cubic local sub-domain Ω_q, whose centre is at the node $\mathbf{x}_i$. The Gauss quadrature rule of an appropriate order is employed to evaluate integrals over each local sub-domain.

3 Stress – strain relation based on deformation theory

The strain–stress relationship can be taken in the form [Jahed, Sethuraman and Dubey (1997)]

$$\varepsilon_{ij} = f(\sigma_{ij}) \tag{36}$$

where f is a function and ε_{ij} is the total strain tensor, which

$$\varepsilon_{ij} = \varepsilon^{\mathrm{e}}_{ij} + \varepsilon^{\mathrm{p}}_{ij} \tag{37}$$

according to the additive decomposition the total strain tensor is the summation of conservative elastic $\varepsilon^{\mathrm{e}}_{ij}$ and nonconservative plastic part $\varepsilon^{\mathrm{p}}_{ij}$. The elastic strain tensor is related to the stress tensor by Hook's law for isotropic materials as;

$$\varepsilon^{\mathrm{e}}_{ij} = \frac{1+\nu}{E}\sigma_{ij} - \frac{\nu}{E}\sigma_{kk}\delta_{ij} \tag{38}$$

The plastic strain tensor is also related to the deviatoric part of stress tensor based on Hencky's total deformation theory as;

$$\varepsilon^{\mathrm{p}}_{ij} = \Psi S_{\mathrm{ij}} \tag{39}$$

Where Ψ is a scalar valued function, given by

$$\Psi = \frac{3\varepsilon^{\mathrm{p}}{}_{equivalent}}{2\sigma_{equivalent}} = \frac{3}{2}\frac{\sqrt{2\varepsilon^{\mathrm{p}}_{ij}\varepsilon^{\mathrm{p}}_{ij}/3}}{\sqrt{3S_{\mathrm{ij}}S_{\mathrm{ij}}/2}} \tag{40}$$

and

$$S_{\mathrm{ij}} = \sigma_{ij} - \frac{1}{3}\sigma_{kk}\delta_{ij} \tag{41}$$

is deviatoric stress tensor. By substituting Eqs. 38–41 into Eq. 37, we can get

$$\varepsilon_{ij} = \left(\frac{1+\nu}{E} + \Psi\right)\sigma_{ij} - \left(\frac{\nu}{E} + \frac{1}{3}\Psi\right)\sigma_{kk}\delta_{ij} \tag{42}$$

Eq. 42 can be rewritten as:

$$\varepsilon_{ij} = \frac{1+\nu_e}{E_e}\sigma_{ij} - \frac{\nu_e}{E_e}\sigma_{kk}\delta_{ij} \tag{43}$$

Where, E_e and ν_e are termed as the effective Young's modulus and the effective Poisson's ratio, respectively, which are functions of E, ν and ψ and are considered as material parameters. By comparing Eq. 42 and 43, effective values of material parameters can be obtained as;

$$E_e = \frac{1}{\left(\frac{1}{E}\right) + \left(\frac{2}{3}\Psi\right)} \tag{44}$$

$$\nu_e = \frac{\left(\frac{\nu}{E}\right) + \left(\frac{\Psi}{3}\right)}{\left(\frac{1}{E}\right) + \left(\frac{2}{3}\Psi\right)} \tag{45}$$

Eq. 43 is the effective constitutive equation for the analysis of material nonlinearity.

4 Determination of the effective material parameters

By employing relations of effective Young's modulus and the effective Poisson's ratio from Eqs. 44 and 45, for different material behaviors containing linear or nonlinear stress-strain relationship, effective material parameters can be obtained.

For example, for the elastic-perfectly plastic material, as shown in Fig. 2, the yield stress is σ_0; we can obtain the effective material parameters as;

$$\frac{1}{{E_e}^{perfect}} = \frac{1}{E} + \frac{\varepsilon^p}{\sigma_0} \tag{46}$$

$${\nu_e}^{perfect} = {E_e}^{perfect}\left(\frac{\nu}{E} + \frac{?^p}{2\sigma_0}\right) \tag{47}$$

For linear work- hardening materials, in which σ_0 is assumed as yield stress and E_T as tangent modulus, the effective material parameters can be obtained as;

$$\frac{1}{{E_e}^{harden}} = \frac{\sigma_0}{E\sigma} + \frac{\sigma - \sigma_0}{\sigma E_T} \tag{48}$$

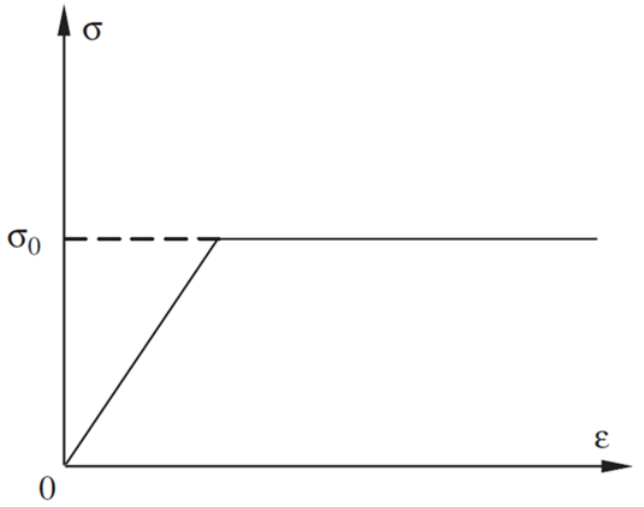

Figure 2: The stress–strain relation for an elastic–perfectly plastic material.

$$\nu_e{}^{harden} = E_e{}^{harden}\left(\frac{\nu}{E} + \frac{\sigma_0 - \sigma}{2\sigma}\left(\frac{1}{E} - \frac{1}{E_T}\right)\right) \tag{49}$$

One general case of hardening material model is Ramberg – Osgood formula which represent the stress – strain relation with power law as shown in Fig. 3. The relation between stress and strain in this model can be written as;

$$\frac{\varepsilon}{\varepsilon_0} = \frac{\sigma}{\sigma_0} + \alpha\left(\frac{\sigma}{\sigma_0}\right)^n \tag{50}$$

where ε_0 is the strain at initial yield, α is the yield offset, and n is the hardening exponent. Both α and n are material constants and are obtained from experimental tests. The effective material parameters can be expressed in the form;

$$\frac{1}{E_e{}^{Ramb}} = \frac{1}{E} + \alpha\frac{\varepsilon_0}{\sigma_0}\left(\frac{\sigma}{\sigma_0}\right)^{n-1} \tag{51}$$

$$\nu_e{}^{Ramb} = E_e{}^{Ramb}\left(\frac{\nu}{E} + \frac{1}{2}\alpha\frac{\varepsilon_0}{\sigma_0}\left(\frac{\sigma}{\sigma_0}\right)^{n-1}\right) \tag{52}$$

The effective material parameters which are presented here are functions of the final state of stress fields. They are also related to the position of a point because

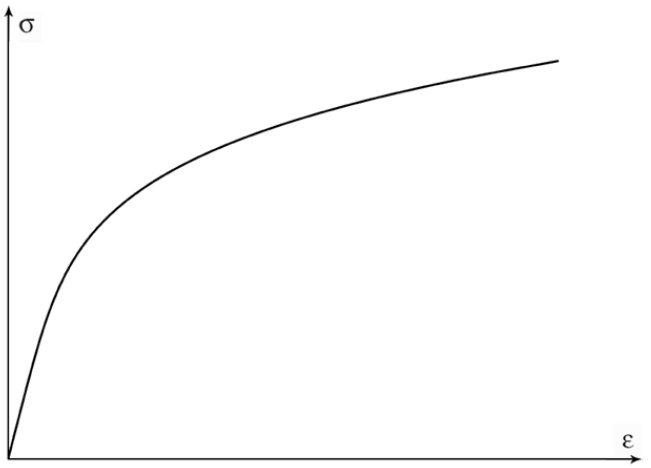

Figure 3: The stress–strain relation for Ramberg – Osgood model.

the stress is also the function of position. Hence, the effective material parameters can be proposed as field variables describing the material properties of each point, where the stress state is unique. On the other hand the system of equations is constructed based on the Gauss quadrature points, and therefore, the effective material parameters should be also calculated for each Gauss quadrature points.

5 Numerical procedure

As mentioned above, the effective material parameters are functions of the final stress fields, which are usually unknown. Hence, the direct method is impossible to get the final solution. Thus, to get solution from Eq. 31, the effective material matrix D_e in Eq. 26 should be calculated at first. In this regard, following iteration method based on the projection technique [Desikn and Sethuraman (2000)] is used.

5.1 Projection technique

In the projection method, initially, a linear elastic MLPG analysis is carried out. Consider a particular material point, and evaluate the equivalent stress from linear elastic analysis. To determine whether a material enters the plastic range, the Von Mises yield criterion in three dimensional space [Owen and Hinton (1980)] , which compares the equivalent stress with the yield stress, is used (see Eq. 53). If this point is in elastic phase, the material parameters will be kept unchanged as elastic one and the material still satisfies the linear elasticity; if mentioned point enters

in plastic phase, it means that the deformation already enters the plastic region, and the following iteration computing will be performed to calculate the effective material parameters. This state is shown as a point 'A' in Fig. 4. This point has crossed the yield stress. Keeping the strain values the same, i.e. strain controlled, and projecting the point 'A' on the experimental uniaxial curve (point 'B'), the effective value of Young's modulus for the next iteration is obtained. Substituting this effective value in Eq. 45 the effective Poisson's ratio is obtained. These effective values are obtained for all the nodal and Gauss points, which have been yielded. With this new set of effective material parameters the next linear elastic MLPG analysis is performed. This iterative procedure is repeated and elastic analysis with currently evaluated E_e and ν_e is performed until all the effective material parameters converge and equivalent stress falls on the experimental uniaxial stress-strain curve. However, if the applied loading is too large, the computing may not converge, and it means that the material is already failure, and this certain loading is called the critical failure loading which is also an important parameter for solids and structures.

$$\sigma_e = \frac{1}{\sqrt{2}}\left[(\sigma_1-\sigma_2)^2+(\sigma_2-\sigma_3)^2+(\sigma_3-\sigma_1)^2\right]^{1/2} \tag{53}$$

$$\begin{cases} \sigma_e < \sigma_y & \textit{the material is elastic} \\ \sigma_e \sigma_y & \textit{the material has yielded} \end{cases}$$

Fig. 5 shows the flowchart of the iterative solution procedure for the governing equations. The iteration criterion is defined as;

$$\sqrt{\frac{\int_{j=1}^{n}\left(E_{ej}{}^{(i+1)}-E_{ej}{}^{(i)}\right)^2}{\int_{j=1}^{n}\left(E_{ej}{}^{(i)}\right)^2}} \le R \tag{54}$$

Where n is the number of quadrature points, $E_e{}^{(i)}$ and $E_e{}^{(i+1)}$ are the effective Young's modulus of ith and $(i+1)$th iteration steps, respectively, and R is a predefined accuracy tolerance.

6 Numerical examples

Gauss quadrature is used to evaluate the integral equations obtained from meshless formulation. For a field node $\mathbf{x}_I$, a local quadrature cell $\Omega_q$is needed for the Gauss quadrature. For each Gauss quadrature point $\mathbf{x}_q$, the MLS shape functions are constructed to obtain the integrand. Because of simplicity, the cubic quadrature domain is used to integrate the integral equations. For node $\mathbf{x}_I$, the size of the

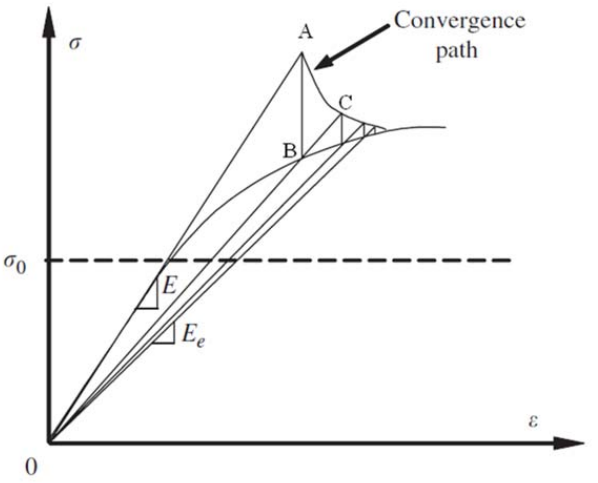

Figure 4: Determination of E_e by the projection method.

quadrature domain can be determined by r_{qx}, $r_{qy}$and r_{qz} in the x, y and z directions, respectively, as follows;

$$\begin{cases} r_{qx} = \alpha_{qx} d_{cx} \\ r_{qy} = \alpha_{qy} d_{cy} \\ r_{qz} = \alpha_{qz} d_{cz} \end{cases} \tag{55}$$

where α_{qx}, α_{qy} and α_{qz} are dimensionless sizes of the local quadrature domain in the x, y and z directions, respectively.

The local support domain for a Gauss quadrature point $\mathbf{x}_q$ can be arbitrary in shape. In this paper, a cubic support domain is used. The size of the local support domain is determined by r_{sx}, r_{sy} and r_{sz} in the x, y and z directions, respectively.

$$\begin{cases} r_{sx} = \alpha_{sx} d_{cx} \\ r_{sy} = \alpha_{sy} d_{cy} \\ r_{sz} = \alpha_{sz} d_{cz} \end{cases} \tag{56}$$

where d_{cx}, d_{cy} and d_{cz} are, respectively, the local nodal spacing in x, y and z directions and α_{sx}, $\alpha_{s?}$ and α_{sz} are dimensionless sizes of the local support domain in the x, y and z directions, respectively.

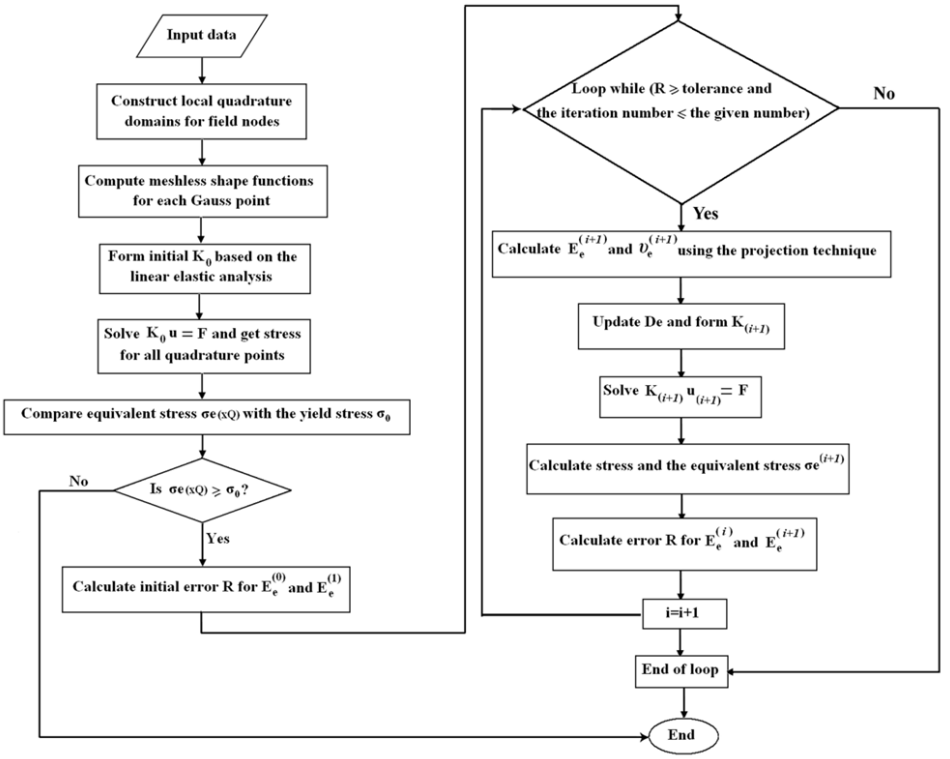

Figure 5: Flowchart of solution procedure.

In this regard, the dimensions of the local quadrature domain and local support domain used for Gauss quadrature and constructing the MLS shape functions become $(2\alpha_{qx}d_{cx}) \times (2\alpha_{qy}d_{cy}) \times (2\alpha_{qz}d_{cz})$ and $(2\alpha_{sx}d_{cx}) \times (2\alpha_{sy}d_{cy}) \times (2\alpha_{sz}d_{cz})$, respectively.

In the present study, for the local support domain, $\alpha_{sx} = \alpha_{sy} = \alpha_{sz} = 2.7$ and for the local quadrature domain, $\alpha_{qx} = \alpha_{qy} = \alpha_{qz} = 0.8$ are used.

Several numerical problems have been analyzed to demonstrate the accuracy and efficiency of the present method. Results obtained from present meshless method are compared with those of finite element solution from ABAQUS.

6.1 Uniaxial tension of a 3D bar

A 3D cantilever bar subjected to a uniformly distributed tensile load, having a resultant F at its end, is analyzed. Geometry and nodal distributions of the bar can be seen in Fig. 6. The Young's modulus, Poisson's ratio and yield stress are as-

sumed as $E=2.1\times10^{11}$ *pa*, $\nu = 0.3$ and $\sigma_0=1.68\times10^8$*pa*, respectively. The material is initially considered as elastic-perfectly plastic. The discretization is performed by $11\times3\times3$ distributed nodes among the problem domain. Fig. 7 and 8 show the convergence paths for different resultant load F in the bar. It can be seen that the present method using the projection technique can quickly produce convergent results. However, the number of iteration steps will increase as F increases. As shown in Fig. 9, when F becomes larger than a certain value, the results will not be converged, and the structure fails. This value is called the critical failure load, and it is $F = 154\times10^5$ *N* in this problem.

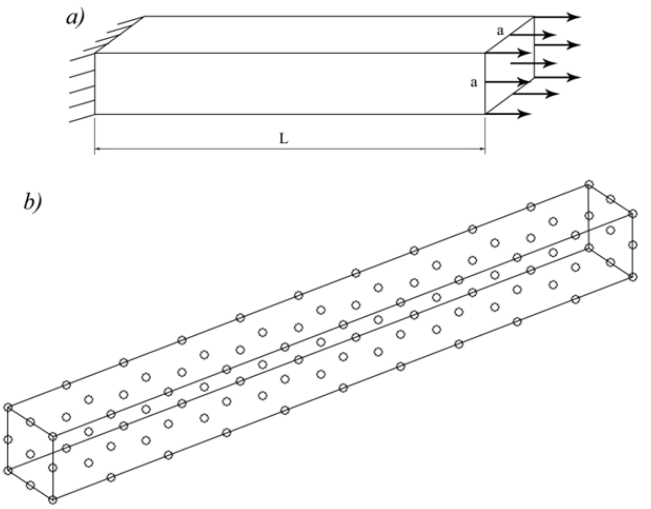

Figure 6: A 3D cantilever bar subjected to a uniformly distributed tensile load: (a) geometry and load conditions, (b) $11\times3\times3$ nodal distribution.

Fig. 10 shows the horizontal displacement of free end of the bar, under different loadings. For comparison, FEM results obtain from ABAQUS are also plotted in the same figure. It can be seen that results obtained from present method are in good agreement with those of FEM.

A work-hardening material based on Ramberg – Osgood model is also considered. As shown in Fig. 11, a work-hardening material with a much higher resultant load than an elastic-perfectly plastic material is rapidly converged.

6.2 3D thick plates subjected to a uniformly distributed load

A 3D thick cantilever plate subjected to a uniformly distributed load is also studied. The plate thickness to span ratio is $h/a=0.1$. The material data are Young's modulus

a)

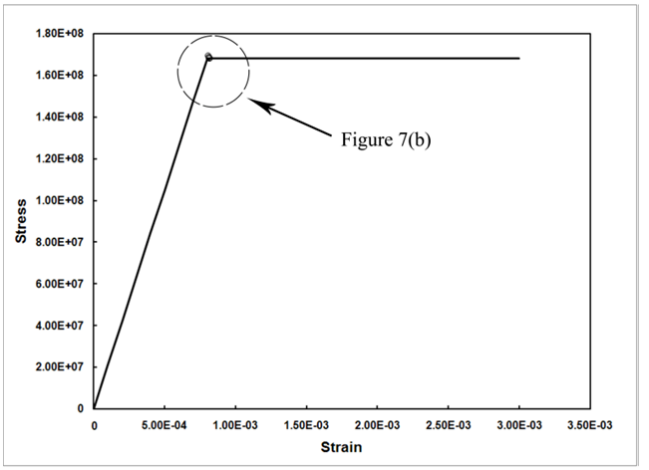

b)

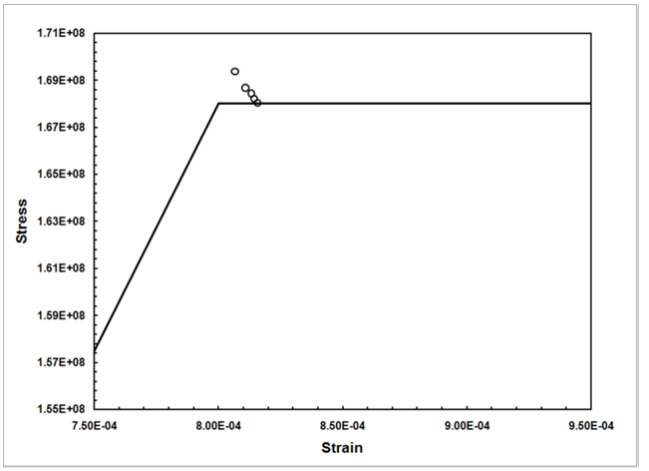

Figure 7: The convergence path of the bar with elastic-perfectly plastic material ($F=152\times10^5N$): (a) the convergence path, (b) the magnified convergence path.

$E=2.1\times10^{11}$ pa, Poisson's ratio $\nu=$ 0.3 and yield stress $\sigma_0=1.7\times10^5 pa$. Due to symmetry, only one half of the plate is discretized by the various uniformly distributed nodal points on the domain of the plate. The discretization by $7\times3\times3$ nodes is shown in Fig. 12.

Fig. 13 shows the deflection of midline of the plate with respect to the plate length. The plate deflections are normalized by its elastic value from analytical solution Srinivas and Rao (1973) and are compared with results obtained from finite element

a)

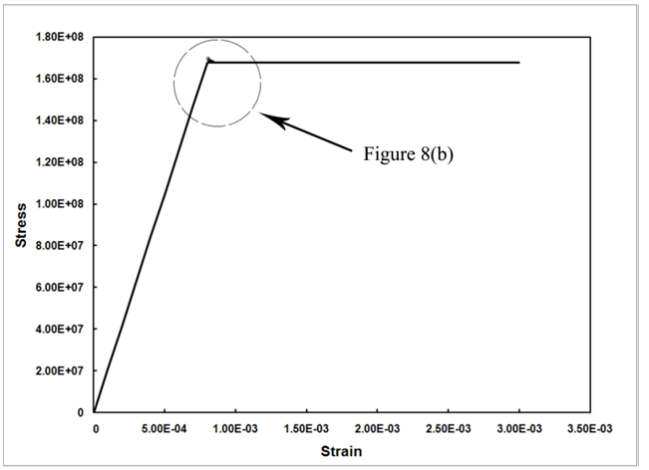

b)

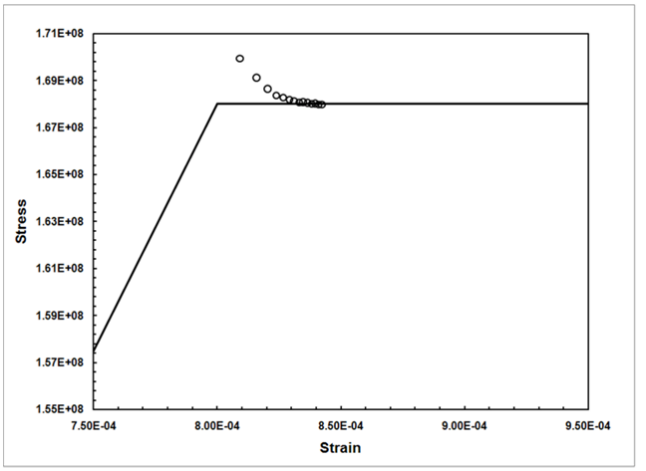

Figure 8: The convergence path of the bar with elastic-perfectly plastic material ($F=153\times10^5$ N): (a) the convergence path, (b) the magnified convergence path.

commercial software ABAQUS. Fig. 14 represents the convergence path of the midpoint on the clamped edge of the plate versus number of iterations.

At last, a fully clamped square plate subjected to a uniformly distributed load is considered. The plate thickness to span ratio is $h/a=0.1$ and its material properties

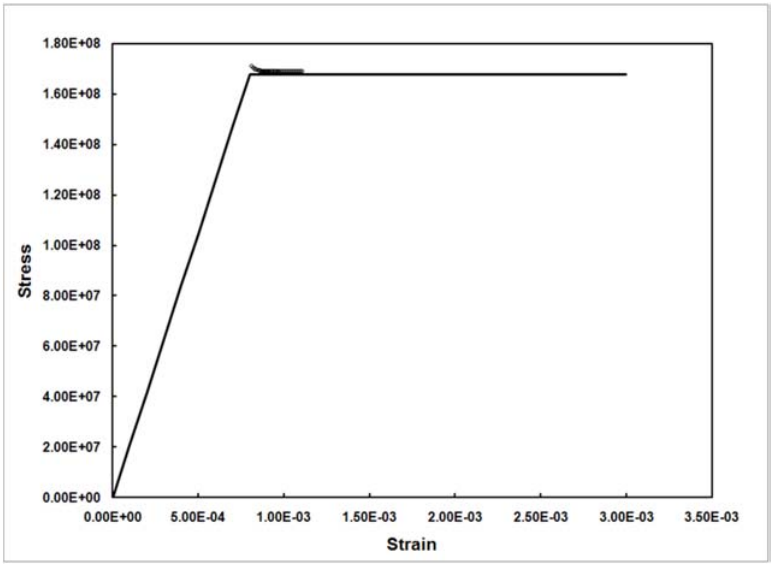

Figure 9: The convergence path of the bar with elastic-perfectly plastic material ($F=154\times10^5 N$).

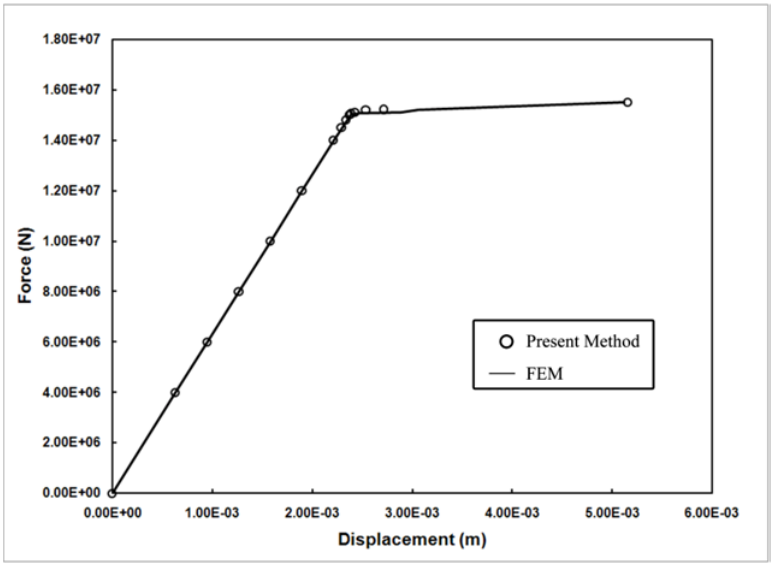

Figure 10: Force-Displacement curve of the bar with elastic-perfectly plastic material.

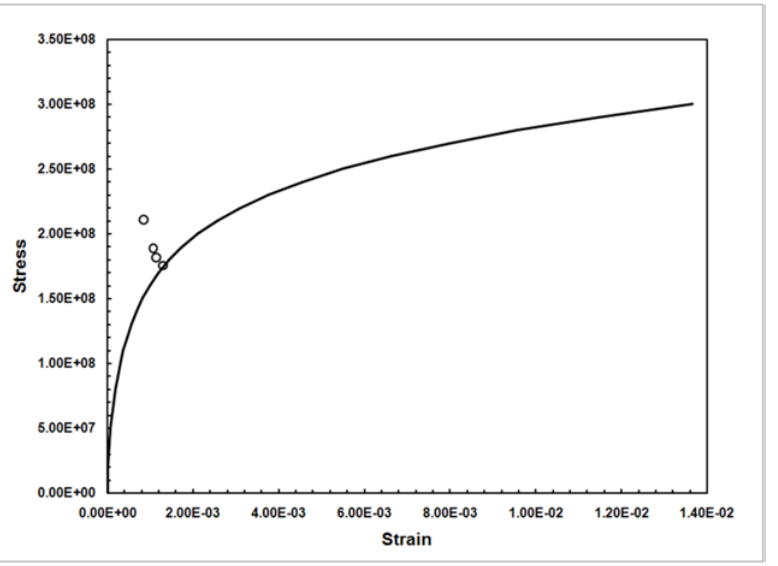

Figure 11: The convergence path of the bar with Ramberg – Osgood material ($F=160\times10^5N$)

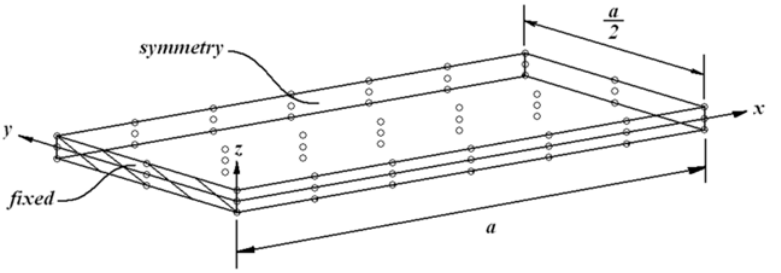

Figure 12: Discretization of one half of the plate with $7\times3\times3$ nodes.

are $E=10\times10^5$, $\nu = 0.3$ and $\sigma_0=2.7\times10^4 pa$. Due to symmetry, only one quarter of the plate is discretized by $7\times7\times3$ nodes on the problem domain and is shown in Fig. 15.

Fig. 16 and 17 present normalized deflection and convergence path of the plate versus plate length and number of iterations, respectively. It can be seen that results obtained from present method are in good agreement with those of finite element solution from ABAQUS.

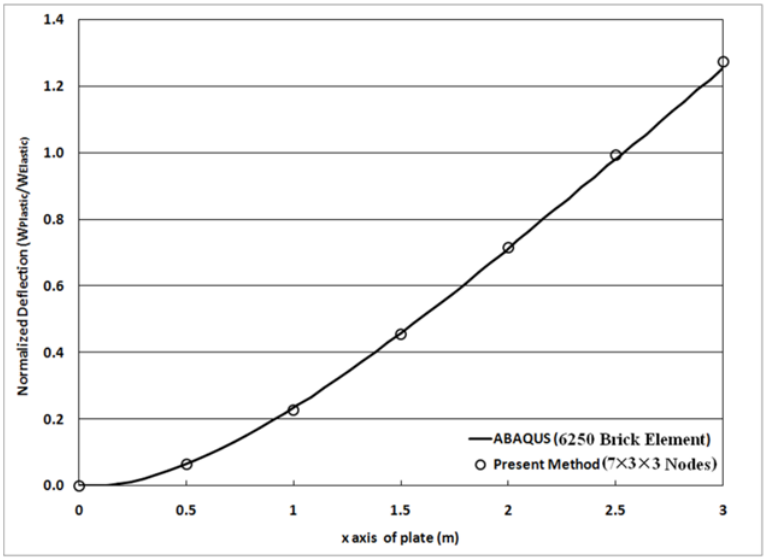

Figure 13: Deflection of midline of the plate versus plate length.

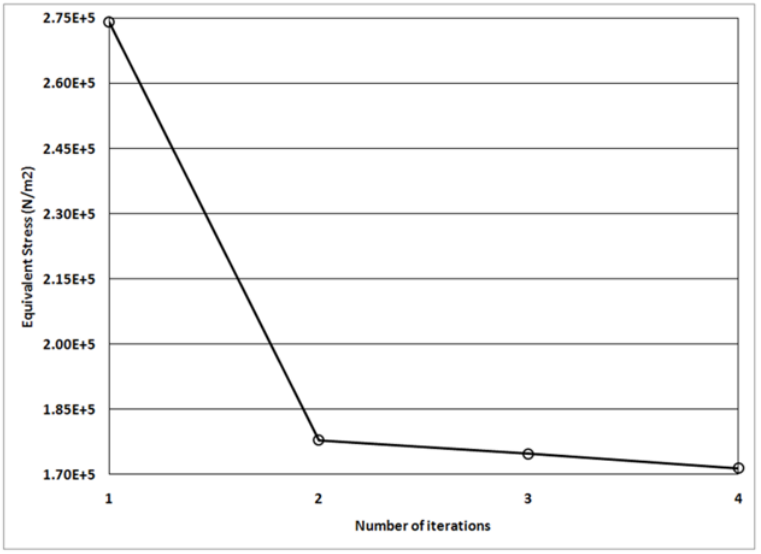

Figure 14: The convergence path of the cantilevered plate.

7 Conclusion

In the present paper, meshless local petrov-galerkin method is developed for 3D elasto-plastic problems. Based on local petrov-galerkin approach, weak form of

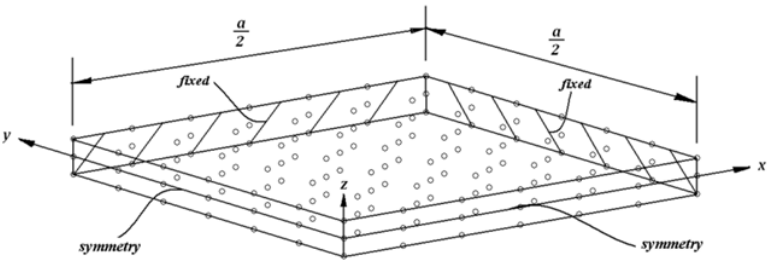

Figure 15: Discretization of one quarter of the plate with $7\times7\times3$ nodes.

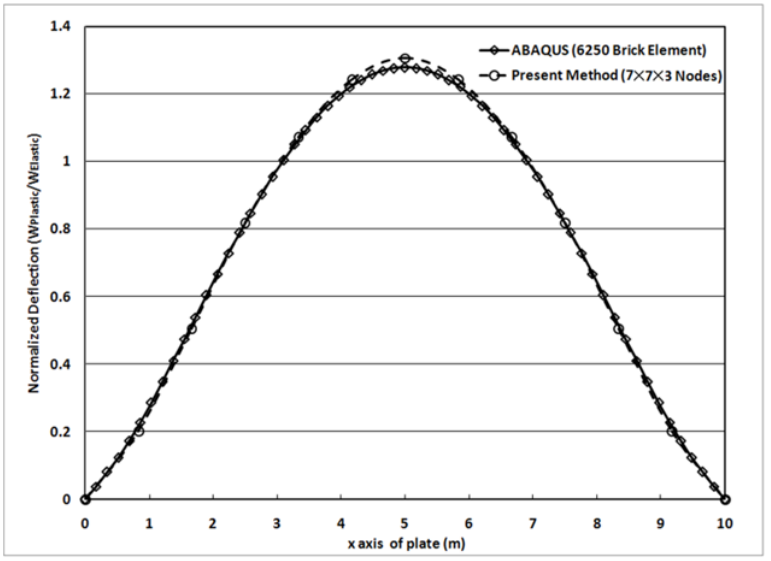

Figure 16: Normalized deflection of the plate versus plate length.

equilibrium equation is obtained. Three dimensional MLS approximation is used as shape function to get the meshless discrete system of equations. Numerical integration is performed using Gauss quadrature method. A weak formulation for the set of governing equations is transformed into local integral equations on local sub-domains by using a unit test function. Nodal points are distributed in the 3D analyzed domain and each node is surrounded by a cubic sub-domain to which a local integral equation is applied. Hencky's total deformation theory is used to define the effective material parameters, which are treated as spatial field variables and considered as functions of the equilibrium stress state and material properties. These effective material parameters are obtained in an iterative manner using strain

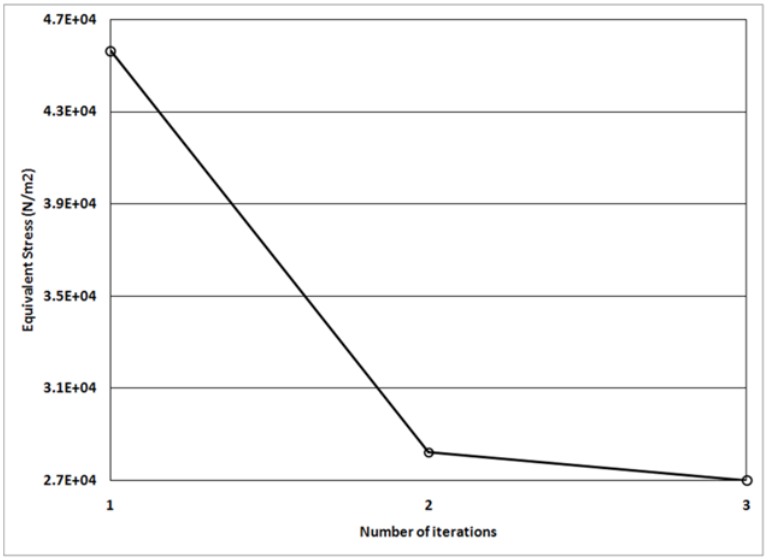

Figure 17: The convergence path of the fully clamped plate.

controlled projection method using experimental uniaxial tension test curve. Von Mises yield criterion in three dimensional space is used as a yield function. The supports of the MLS approximation function cover the same sets of nodes during iterative procedures, thus the shape function need to be computed only in the initial stage. Several numerical examples are presented to illustrate the effectiveness of present formulation for the elasto-plastic analysis of 3D solids. It has been found that this meshless method is very effective with rapid convergence for problems with material nonlinearities.

Reference

Atluri, S. N.; Cho, J. Y.; Kim, H. G. (1999): Analysis of thin beams, using the meshless local Petrov–Galerkin method, with generalized moving least squares interpolations. *CMES: Computer Modeling in Engineering & Sciences*, vol. 24, no. pp. 334-347.

Atluri, S. N.; Kim, H. G.; Cho, J. Y. (1999): A critical assessment of the truly meshless local Petrov–Galerkin (MLPG), and local boundary integral equation (LBIE) methods. *Comput. Mech.*, vol. 24, no. pp. 348-372.

Atluri, S. N.; Shen, S. (2002a): The meshless local Petrov-Galerkin (MLPG) method: A simple & less costly alternative to the finite element and boundary ele-

ment methods. *CMES: Computer Modeling in Engineering & Sciences*, vol. 3, no. pp. 11-52.

Atluri, S. N.; Shen, S. (2002b): *The Meshless Local Petrov–Galerkin (MLPG) Method*. Tech Science Press.

Atluri, S. N.; Zhu, T. (1998): A new meshless local Petrov–Galerkin (MLPG) approach in computational mechanics. *Comput. Mech.*, vol. 22, no. pp. 117-127.

Atluri, S. N.; Zhu, T. (2000): The meshless local Petrov–Galerkin (MLPG) approach for solving problems in elasto-statics. *Comput. Mech.*, vol. 25, no. pp. 169-179.

Babuska, I.; Melenk, J. (1997): The partition of unity method. *Int. J. Numer. Methods Engrg.*, vol. 40, no. pp. 727–758.

Batra, R. C.; Ching, H. K. (2002): Analysis of elastodynamic deformation near a crack/ notch tip by the meshless local Petrov–Galerkin (MLPG) Method. *CMES: Computer Modeling in Engineering & Sciences*, vol. 3, no. pp. 717-730.

Belinha, J.; Dinis, L. M. J. S. (2006): Elastoplastic analysis of plates by the element free Galerkin method. *Int. J. Comput.-Aided Engrg. Software*, vol. 23, no. 5, pp. 525-551.

Belytschko, T.; Liu, W. K.; Moran, B. (2000): *Nonlinear finite elements for continua and structures*. Wiley.

Belytschko, T.; Lu, Y. Y.; Gu, L. (1994): Element-free Galerkin methods. *Int. J. Numer. Methods Engrg.*, vol. 37, no. pp. 229-256.

Chen, J. S.; Pan, C.; Wu, C. T.; Liu, W. K. (1996): Reproducing Kernel Particle Methods for large deformation analysis of non-linear structures. *Comput. Methods Appl. Mech. Engrg.*, vol. 139, no. pp. 195-227.

Chen, Y. P.; Lee, J. D.; Eskandarian, A. (2002): Dynamic meshless method applied to nonlocal crack problems. *Theor. Appl. Mech.*, vol. 38, no. pp. 293–300.

Ching, H. K.; Batra, R. C. (2001): Determination of crack tip fields in linear elastostatics by the meshless local Petrov–Galerkin (MLPG) method. *CMES: Computer Modeling in Engineering & Sciences*, vol. 2, no. pp. 273-290.

Ching, H. K.; Yen, S. C. (2005): Meshless local Petrov-Galerkin analysis for 2D functionally graded elastic solids under mechanical and thermal loads. *Composites: Part B*, vol. 36, no. pp. 223-240.

Ching, H. K.; Yen, S. C. (2006): Transient thermoelastic deformations of 2-D functionally graded beams under nonuniformly convective heat supply. *Compos. Struct*, vol. 73, no. pp. 381-393.

Desikn, V.; Sethuraman, R. (2000): Analysis of material nonlinear problems us-

ing pseudo-elastic finite element method. *J. Press. Vess. Technol.*, vol. 122, no. pp. 457-61.

Duarte, C. A.; Oden, J. T. (1996): An h–p adaptive method using clouds. *Comput. Methods Appl. Mech. Engrg.* , vol. 139, no. pp. 237–262.

Gilhooley, D. F.; Batra, R. C.; Xiao, J. R.; McCarthy, M. A.; Gillespie Jr., J. W. (2007): Analysis of thick functionally graded plates by using higher-order shear and normal deformable plate theory and MLPG method with radial basis functions. *Compos. Struct*, vol. 80, no. pp. 539-552.

Gu, Y. T.; Liu, G. R. (2001): A meshless local Petrov–Galerkin (MLPG) formulation for static and free vibration analyses of thin plates. *CMES: Computer Modeling in Engineering & Sciences*, vol. 2, no. pp. 463-476.

Gu, Y. T.; Wang, Q. X.; Lam, K. Y.; Dai, K. Y. (2007): A pseudo-elastic local meshless method for analysis of material nonlinear problems in solids. *Eng. Anal. Bound. Elem.*, vol. 31, no. pp. 771-782.

Han, Z. D.; Atluri, S. N. (2003): Truly Meshless Local Petrov-Galerkin (MLPG) Solutions of Traction & Displacement BIEs. *CMES: Computer Modeling in Engineering & Sciences*, vol. 4, no. pp. 665-678.

Han, Z. D.; Atluri, S. N. (2004a): A Meshless Local Petrov-Galerkin (MLPG) Approach for 3-Dimensional Elasto-dynamics. *CMC: Comput. Mater. Con.*, vol. 1, no. pp. 129-140.

Han, Z. D.; Atluri, S. N. (2004b): Meshless Local Petrov-Galerkin (MLPG) approaches for solving 3D Problems in elasto-statics. *CMES: Computer Modeling in Engineering & Sciences*, vol. 6, no. pp. 168-188.

Han, Z. D.; Rajendran, A. M.; Atluri, S. N. (2005): Meshless Local Petrov-Galerkin (MLPG) Approaches for Solving Nonlinear Problems with Large Deformations and Rotations. *CMES: Computer Modeling in Engineering & Sciences*, vol. 10, no. pp. 1-12.

Jahed, H.; Sethuraman, R.; Dubey, R. N. (1997): A variable material property approach for solving elastic–plastic problems. *Int. J. Pre. Ves. Piping*, vol. 71, no. pp. 285-291.

Kargarnovin, M. H.; Toussi, H. E.; Fariborz, S. J. (2004): Elasto-plastic element-free Galerkin method. *Comput. Mech.*, vol. 33, no. pp. 206–214.

Kim, H. G.; Atluri, S. N. (2000): Arbitrary placement of secondary nodes, and error control, in the meshless local Petrov–Galerkin (MLPG) method. *CMES: Computer Modeling in Engineering & Sciences*, vol. 1, no. pp. 11-32.

Li, Q.; Shen, S.; Han, Z. D.; Atluri, S. N. (2003): Application of Meshless Local Petrov-Galerkin (MLPG) to Problems with Singularities, and Material Discontinu-

ities, in 3-D Elasticity. *CMES: Computer Modeling in Engineering & Sciences*, vol. 4, no. pp. 567-581.

Li, Q.; Soric, J.; Jarak, T.; Atluri, S. N. (2005): A locking-free meshless local Petrov–Galerkin formulation for thick and thin plates. *J. Comput. Phys.*, vol. 208, no. pp. 116-133.

Li, S.; Hao, W.; Liu, W. K. (2000): Numerical simulations of large deformation of thin shell structures using meshfree methods. *Comput. Mech.*, vol. 25, no. pp. 102-116.

Liew, K. M.; Wu, Y. C.; Zou, G. P.; Ng, T. Y. (2002): Elasto-plasticity revisited: numerical analysis via reproducing kernel particle method and parametric quadratic programming. *Int. J. Numer. Methods Engrg*, vol. 55, no. pp. 669-683.

Lin, H.; Atluri, S. N. (2000): Meshless local Petrov–Galerkin (MLPG) method for convection-diffusion problems. *CMES: Computer Modeling in Engineering & Sciences*, vol. 1, no. pp. 45-60.

Lin, H.; Atluri, S. N. (2001): The meshless local Petrov–Galerkin (MLPG) method for solving incompressible Navier–Stokes equations. *CMES: Computer Modeling in Engineering & Sciences*, vol. 2, no. pp. 117-142.

Liu, T.; Liu, G.; Wang, Q. (2006): An elemen-free Galerkin-finite element coupling method for elastoplastic contact problem. *J. Tribol.*, vol. 128, no. pp. 1–9.

Liu, W. K.; Jun, S.; Zhang, Y. (1995): Reproducing kernel particle methods. *Int. J. Numer. Methods in Fluids*, vol. 20, no. pp. 1081-1106.

Long, S.; Atluri, S. N. (2002): A meshless local Petrov–Galerkin (MLPG) method for solving the bending problem of a thin plate. *CMES: Computer Modeling in Engineering & Sciences*, vol. 3, no. pp. 53-64.

Long, S. Y.; Liu, K. Y.; Li, G. Y. (2008): An analysis for the elasto-plastic fracture problem by the meshless local Petrov-Galerkin method. *CMES: Computer Modeling in Engineering & Sciences*, vol. 28, no. pp. 203-216.

Lucy, L. B. (1977): A numerical approach to the testing of the fission hypothesis. *Astronom. J.*, vol. 82, no. pp. 1013–1024.

Ma, J.; Xin, X. J.; Krishnaswami, P. (2008): Elastoplastic meshless integral method. *Comput. Methods Appl. Mech. Engrg.*, vol. 197, no. pp. 4777-4788.

Nayroles, B.; Touzot, G.; Villon, P. (1992): Generalizing the finite element method: diffuse approximation and diffuse elements. *Comput. Mech.* , vol. 10, no. pp. 307–18.

Owen, D. R. J.; Hinton, E. (1980): *Finite elements in plasticity: theory and practice*. Pineridge Press Limited.

Qian, L. F.; Batra, R. C.; Chen, L. M. (2003): Elastostatic Deformations of a Thick Plate by using a Higher-Order Shear and Normal Deformable Plate Theory and two Meshless Local Petrov-Galerkin (MLPG) Methods. *Comput. Modeling Eng. Sci.*, vol. 4, no. pp. 161-175.

Qian, L. F.; Batra, R. C.; Chena, L. M. (2004): Static and dynamic deformations of thick functionally graded elastic plates by using higher-order shear and normal deformable plate theory and meshless local Petrov–Galerkin method. *Composites: Part B*, vol. 35, no. pp. 685-697.

Rao, B. N.; Rahman, S. (2004): An enriched meshless method for non-linear fracture mechanics. *Int. J. Numer. Methods Engrg.*, vol. 59, no. pp. 197–223.

Rezaei Mojdehi, A.; Darvizeh, A.; Basti, A.; Rajabi, H. (2011): Three dimensional static and dynamic analysis of thick functionally graded plates by the meshless local Petrov–Galerkin (MLPG) method. *Eng. Anal. Bound. Elem.*, vol. 35, no. pp. 1168-1180.

Sladek, J.; Sladek, V.; Atluri, S. N. (2001): A pure contour formulation for the meshless local boundary intergral equation method in thermoelasticity. *CMES: Computer Modeling in Engineering & Sciences*, vol. 2, no. pp. 423-433.

Sladek, J.; Sladek, V.; Krivacek, J.; Wen, P. H.; Zhang, C. h. (2007): Meshless local Petrov–Galerkin (MLPG) method for Reissner–Mindlin plates under dynamic load. *Comput. Methods Appl. Mech. Engrg.*, vol. 196, no. pp. 2681-2691.

Sladek, J.; Sladek, V.; Solek, P. (2009): Elastic analysis in 3D anisotropic functionally graded solids by the MLPG. *Comput. Methods Appl. Mech. Engrg.*, vol. 43, no. pp. 223-251.

Sladek, J.; Sladek, V.; Zhang, C. h. (2005): Stress analysis in anisotropic functionally graded materials by the MLPG method. *Eng. Anal. Bound. Elem.*, vol. 29, no. pp. 597-609.

Soares, D.; Sladek, J.; Sladek, V. (2009): Dynamic Analysis by Meshless Local Petrov-Galerkin Formulations Considering a Time-Marching Scheme Based on Implicit Green's Functions. *CMES: Computer Modeling in Engineering & Sciences*, vol. 50, no. pp. 115-140.

Soric, J.; Li, Q.; Jarak, T.; Atluri, S. N. (2004): Meshless Local Petrov-Galerkin (MLPG) Formulation for Analysis of Thick Plates. *CMES: Computer Modeling in Engineering & Sciences*, vol. 6, no. pp. 349-357.

Srinivas, S.; Rao, A. K. (1973): Flexure of Thick Rectangular Plates. *J. App. Mech. ASME*, vol. 40, no. pp. 298-299.

Sukumar, N.; Moran, B.; Belytschko, T. (1998): The natural element method in solid mechanics. *Int. J. Numer. Methods Engrg.*, vol. 43, no. pp. 839–887.

Tang, Z.; Shen, S.; Atluri, S. N. (2003): Analysis of materials with strain-gradient effects: A meshless local Petrov–Galerkin (MLPG) approach, with nodal displacements only. *CMES: Computer Modeling in Engineering & Sciences*, vol. 4, no. pp. 177-196.

Wendland, H. (1995): Piecewise polynomial positive definite and compactly supported radial basis functions of minimal degree. *Adv. Comput. Methods*, vol. 4, no. pp. 389–396.

Xiao, J. R.; Batra, R. C.; Gilhooley, D. F.; Gillespie Jr., J. W.; McCarthy, M. (2007): Analysis of thick plates by using a higher-order shear and normal deformable plate theory and MLPG method with radial basis functions. *Comput. Methods Appl. Mech. Engrg.*, vol. 196, no. pp. 979-987.

Xu, Y.; Saigal, S. (1998): Element free Galerkin study of steady quasi-static crack growth in plane strain tension in elastic–plastic materials. *Comput. Mech.*, vol. 22, no. pp. 206–214.

Xu, Y.; Saigal, S. (1999): An element-free Galerkin analysis of steady dynamic growth of a mode I crack in elastic–plastic materials. *Int. J. Solids Struct.*, vol. 36, no. pp. 1045–1079.

Zhang, G. M.; Batra, R. C. (2004): Modified smoothed particle hydrodynamics method and its application to transient problems. *Comput. Mech.*, vol. 34, no. pp. 137- 46.

Zhang, X.; Zhenhan, Y.; Zhangfei, Z. (2006): Application of MLPG in large deformation analysis. *Acta Mech. Sin.*, vol. 22, no. pp. 331-340.

Zienkiewicz, O. C.; Taylor, R. L. (2000): *The finite element method*. Butterworth Heinemann.